PINK1 Phosphorylates Drp1^{S616} to Improve Mitochondrial Fission and Inhibit the Progression of HFpEF

Jian Shou
Shanghai Jiaotong University: Shanghai Jiao Tong University
Yunlong Huo (huoyunlong@sjtu.edu.cn)
Shanghai Jiaotong University: Shanghai Jiao Tong University

Research

Keywords: Drp1, HFpEF, Mitochondrial Fission, PINK1

Posted Date: June 7th, 2022

DOI: https://doi.org/10.21203/rs.3.rs-1641454/v1

Abstract

Background: Heart failure with preserved ejection fraction (HFpEF) is a major subtype of HF with no effective treatments. Mitochondrial dysfunctions relevant to the imbalance of fusion and fission occur in HFpEF. The aim of the study is to investigate molecular mechanisms of mitochondrial dysfunctions in HFpEF.

Methods and Results: The HFpEF model was established by feeding Dahl/SS rats with high salt, showing risk factors such as hypertension, mitochondrial dysfunctions and so on. Physiological and biological measurements showed a decrease in the expression of mitochondrial function related genes, ATP production, and mitochondrial fission index in HFpEF. PINK1 knockout in H9C2 cardiomyocytes also showed the same effects. Moreover, PINK1 myocardium-specific overexpression to HFpEF rats activated the $Drp1^{S616}$ phosphorylation and enhanced the mitochondrial fission to slow the progression of HFpEF.

Conclusions: PINK1 can phosphorylate $Drp1^{S616}$ to improve mitochondrial fission, relieve mitochondrial dysfunctions and slow the progression of HFpEF, which highlights the potential treatment of HFpEF.

Introduction

Heart failure (HF) is a complex syndrome with systolic or diastolic dysfunctions [1]. This reduces the blood pumping capacity of the heart and cannot achieve the metabolic needs of human organs and tissues. Heart failure with reduced ejection fraction (HFrEF) and heart failure with preserved ejection fraction (HFpEF) are two main subtypes of HF [2, 3]. The prevalence of HFpEF increases continuously and will become predominant in China [4]. The risk factors of HFpEF include diabetes, obesity, hypertension and so on, showing diastolic dysfunctions, myocardial hypertrophy, interstitial fibrosis and other phenotypes [3, 5–7]. Substantial mitochondria in myocytes are of importance to regulate HFpEF [8, 9]. The risk factors of HFpEF could induce mitochondrial dysfunctions [10].

The balance of fusion and fission maintains the mitochondrial function [11, 12]. The fusion depends on mitofusin 1/2 (Mfn1/2) and optical atrophy 1 (OPA1) to enhance the respiratory capacity of mitochondria [13]. The fission is mainly completed through the dynamic related protein 1 (Drp1) to remove damaged parts [14]. Drp1 is transferred to the outer membrane of mitochondria[15] and binds to mitochondrial fission factor (MFF) and fission protein 1 (Fis1) to promote mitochondrial fission [16, 17]. PTEN induced putative kinase 1 (PINK1), a serine/threonine protein kinase in mitochondria and cytoplasm [18–22], could directly phosphorylate $Drp1^{S616}$ to regulate mitochondrial fission [23]. There are, however, lack of studies to show how PINK1 phosphorylates $Drp1^{S616}$ to regulate the change of mitochondria during the occurrence and development of HFpEF.

The aim of the study is to investigate molecular mechanisms of mitochondrial dysfunctions in HFpEF as well as regulatory effects of PINK1 on mitochondrial fission. Here, we hypothesize that PINK1

phosphorylates Drp1^{S616} to improve mitochondrial fission, relieve mitochondrial dysfunctions and slow the progression of HFpEF. To test the hypothesis, Dahl/SS rats were fed with a HS diet to develop HFpEF. Physiological and biological experiments were carried out during the development of HFpEF. The significance and implications of the study were discussed for the treatment of HFpEF.

Results

HFpEF model

Figures 1A-D show the significant increase of heart weight, LV weight and their ratio to body weight in the HF group. Figures 1F-I show the increase of IVSd and E/E' and the decrease of LVIDd, EDV and E/A, denoting LV diastolic dysfunction in the HF group. There is no statistical difference of EF and FS between control and HF groups. Figures 1L-O showed myocyte hypertrophy and aggravation of interstitial fibrosis in the HF group.

Mitochondrial dysfunctions in HFpEF

To investigate the changes of mitochondria, Fig. 2A shows the relevant genes, i.e., citrate synthase (CS), succeed dehydrogenase (SDH), pyruvate dehydrogenase (PDH), ATP synthase (ATPase), Sirtuin 3 (SIRT3), peroxisome promoter activated receptor gamma coactivator-1 α (PGC-1α) and nuclear respiratory factor-1 (NRF-1) expressions, which decrease significantly in the HF group. There is also a decrease of ATP content, as shown in Fig. 2B. This denotes mitochondrial dysfunctions in HFpEF rats. Figure 2C shows representative images of mitochondrial transmission electron microscopy. The mitochondria change from the round shape to the longer/irregular shape in the HF group. The number of mitochondria decreases and the area increases due to HFpEF (Figs. 2D and E). Accordingly, Figs. 2F and G show a decrease of mitochondrial fission index and mRNA expression of Drp1 despite of no significant changes in mRNA expression of Mfn2.

pDrp1^{S616}-mediated mitochondrial fission

To further determine the changes and mechanisms of mitochondrial fission, Fig. 3A shows the decreased phosphorylation level of Drp1^{S616} in the HF group than the shams albeit there is no statistical difference of total protein content of Drp1. After mitochondrial and cytoplasmic proteins were separated, Fig. 3B shows the decreased level of Drp1 on mitochondria, but the increased level of Drp1 in the cytoplasm in the HF group, which denotes the reduced mitochondrial localization of Drp1. Figures 3C and D show the reduced co-localization of Drp1 and mitochondria in myocytes of HFpEF rats. Hence, the mitochondrial fission is reduced by HFpEF.

PINK1-regulated mitochondrial fission

The regulation of Drp1 by PINK1 (an upstream factor of Drp1) was investigated in Fig. 4 for understanding the changes of mitochondrial fission in HFpEF. Figures 4A and B show the significant decrease of PINK1 mRNA and protein levels in the LV of HF rats. Moreover, PINK1 was knocked out in

H9C2 cardiomyocytes, which reduces the phosphorylation level of $Drp1^{S616}$ significantly despite of no significant change in the total protein content of Drp1, as shown in Figs. 4C and D. Figures 4E and F show the decreased content of Drp1 on mitochondria and the increased content of Drp1 in cytoplasm, consistent with the findings in Fig. 3. Figure 4G shows representative images of immunofluorescence of H9C2 cardiomyocytes. The co-localization degree of Drp1 and mitochondria decreases, as shown in Fig. 4H. Representative images of Mito-Tracker Red fluorescent staining of mitochondrial morphology show the change of mitochondria from a round shape to a longer shape after PINK1 knockout in Fig. 4I while the mitochondrial aspect ratio increases in Fig. 4J. Hence, PINK1 knockout leads to the decrease of $Drp1^{S616}$ phosphorylation-mediated mitochondrial fission. Figures 4K-N show the decrease of the expression of mitochondrial function related genes (CS, SDH, PDH, ATPase and PGC-1α), mitochondrial membrane potential, and ATP content after PINK1 knockout, which denotes mitochondrial dysfunctions.

$pDrp1^{S616}$-mediated mitochondrial fission regulates mitochondrial function

To confirm whether mitochondrial dysfunctions after PINK1 knockout is caused by the decrease of $Drp1^{S616}$ phosphorylation-mediated mitochondrial fission, wild-type Drp1 ($Drp1^{WT}$) and phosphorylated mutant Drp1 ($Drp1^{S616A}$) were overexpressed on the basis of $PINK1^{KO}$ cardiomyocytes. This significantly increased the total protein content of Drp1 while the overexpression of $Drp1^{WT}$, rather than $Drp1^{S616A}$, increased the phosphorylation level of $Drp1^{S616}$ (Fig. 5A). The overexpression of $Drp1^{WT}$ also significantly increased the content of Drp1 on mitochondria and reversed the effect of PINK1 knockout despite of no changes owing to overexpression of $Drp1^{S616A}$, as shown in Figs. 5B and C. The overexpression of $Drp1^{WT}$ increases the co-localization degree of Drp1 and mitochondria while overexpression of $Drp1^{S616A}$ reduces it, as shown in Figs. 5D and E. Hence, the mitochondrial localization of Drp1 is mainly caused by the phosphorylation of Drp1 S616 site. Accordingly, the change in the mitochondrial morphometry in Figs. 5K and L shows that phosphorylation of Drp1 S616 site regulates mitochondrial fission. On the other hand, Figs. 5F-J show that overexpression of $Drp1^{WT}$ but not overexpression of $Drp1^{S616A}$, increases the expression of mitochondrial function-related genes (CS, SDH, PDH, ATPase, PGC-1α), mitochondrial membrane potential, and ATP content, and reverses the effect of PINK1 knockout, which denotes that $Drp1^{S616}$ phosphorylation can directly regulate mitochondrial function. These results supported that $Drp1^{S616}$ phosphorylation promotes mitochondrial localization of Drp1 and improves mitochondrial fission to relieve mitochondrial dysfunctions.

PINK1 improves HFpEF phenotypes

To investigate the effects of PINK1 on HFpEF, PINK1 myocardium-specific overexpression was caused by AAV transfection to the HP group. Figure 6 shows that PINK1 overexpression can prevent myocardial hypertrophy, aggravation of interstitial fibrosis and diastolic dysfunctions to slow the progression of HFpEF.

PINK1 stimulates pDrp1^{S616}-mediated mitochondrial fission for improvement of mitochondrial function

We studied whether the improvement of PINK1 on HFpEF was related to Drp1^{S616} phosphorylation-mediated mitochondrial fission and mitochondrial function. In comparison with the HF group, Figs. 7A and B show the increase of phosphorylation level of Drp1^{S616} and PINK1 mRNA expression as well as the relative unchanged total protein content of Drp1; Figs. 7C and D show the increased content of Drp1 on the mitochondria and the decreased content of Drp1 in the cytoplasm; Fig. 7E and F show the higher co-localization degree of Drp1 and mitochondria in the HP group. Transmission electron microscope images also show the increased number and the decreased area of mitochondria (Figs. 7G-J). Hence, PINK1 overexpression improves mitochondrial fission in HF rats. Moreover, Figs. 7K and L show the increased expression of mitochondrial function-related genes (CS, SDH, PDH, ATPase, PGC-1α) and ATP content in the HP group. PINK1 overexpression activates the Drp1^{S616} phosphorylation-mediated mitochondrial fission to improve the mitochondrial function.

Discussion

This study investigated the molecular mechanisms of mitochondrial dysfunctions in HFpEF relevant to the regulatory effect of PINK1. The findings were reported as: (1) HFpEF impaired mitochondrial fission and led to mitochondrial dysfunctions; (2) In H9C2 cardiomyocytes, PINK1 knockout decreased the phosphorylation level of Drp1^{S616} and the mitochondrial localization of Drp1, inhibited the mitochondrial fission, and induced the mitochondrial dysfunctions. (3) In HFpEF rats, PINK1 myocardium-specific overexpression activated the Drp1^{S616} phosphorylation, enhanced the mitochondrial fission, and slowed the progression of HFpEF.

The HFpEF model was established by feeding Dahl/SS rats with high salt, showing risk factors such as hypertension, myocardial hypertrophy, diastolic dysfunctions and interstitial fibrosis, consistent with previous studies [3, 24–26]. Mitochondrial dysfunctions occurred during the occurrence and progression of HFpEF [27], which was caused by the imbalance between mitochondrial fusion and fission [28]. This study showed a decrease in the expression of mitochondrial respiratory function related genes, ATP production, and mitochondrial fission index as well as the altered mitochondrial morphometry, which characterized mitochondrial dysfunctions in HFpEF rats.

Phosphorylating the Ser616 site of Drp1 is transferred to the mitochondrial outer membrane and bound to receptors, i.e., MFF and Fis1, to stimulate mitochondrial fissions [16]. We showed a decrease in the phosphorylation level of Drp1^{S616} and the mitochondrial localization of Drp1, which impaired mitochondrial fissions and induced mitochondrial dysfunction in HFpEF rats. Although elongated mitochondria with larger area become more conducive to enhance mitochondrial function and promote ATP production [28], the over fused mitochondria without fission cannot remove damaged parts and hence induce HFpEF, consistent with studies of Shengnan Wu et al. [29] and Akihiro Shirakabe et al. [30].

PINK1, a serine/threonine protein kinase, is known to phosphorylate $Drp1^{S616}$ [23]. In H9C2 cardiomyocytes, PINK1 knockout reduced the phosphorylation level of $Drp1^{S616}$ and the mitochondrial localization of Drp1. This resulted in a decrease in mitochondrial fission capacity and an increase in mitochondrial aspect ratio in agreement with the study of Hailong Han et al. [23]. On the other hand, PINK1 knockout decreased the expression of mitochondrial function related genes, mitochondrial membrane potential, and ATP production, showing mitochondrial dysfunctions. Moreover, in PINK1 knockout cells, overexpression of $Drp1^{WT}$, but not overexpression of $Drp1^{S616A}$, improved mitochondrial functions. The findings indicated the missing regulation of Drp1 on mitochondrial fission and mitochondrial function when the S616 site of Drp1 was not phosphorylated. Hence, PINK1 phosphorylates $Drp1^{S616}$ to improve mitochondrial fission and restore mitochondrial function.

Myocardial-specific overexpression of PINK1 was achieved in HFpEF rats by AAV. The phosphorylation level of $Drp1^{S616}$ and the mitochondrial localization of Drp1 increased in HFpEF rats after PINK1 overexpression. PINK1 overexpression also restored myocardial functions and reduced the degree of interstitial fibrosis. Hence, PINK1 myocardium-specific overexpression activated the $Drp1^{S616}$ phosphorylation and enhanced the mitochondrial fission such that it slowed the progression of HFpEF, as shown in Fig. 8.

Critiques of the study:

Although regulatory mechanism of PINK1/$Drp1^{S616}$/mitochondrial pathway on HFpEF was showed, the upstream of PINK1 is still unknown. Recent studies have shown that mitochondrial PINK1 expression in nucleus pulposus cells is significantly inhibited under high stress conditions [31]. In the hypertension-induced HFpEF rats, heart and cardiomyocytes were continuously subjected to high stress. The high myocardial stress stimulated the decrease of PINK1 expression. There is a lack of technologies targeting PINK1 for HFpEF, which require further investigations.

Conclusions

We carried out physiological and biological experiments in HFpEF rats. HFpEF caused mitochondrial dysfunctions relevant to the impairment of mitochondrial fission. PINK1 knockout in H9C2 cardiomyocytes also impaired mitochondrial fission and functions. Furthermore, PINK1 myocardium-specific overexpression to HFpEF rats was found to activate the $Drp1^{S616}$ phosphorylation and enhance the mitochondrial fission, which slowed the progression of HFpEF. Hence, PINK1 can phosphorylate $Drp1^{S616}$ to improve mitochondrial fission, relieve mitochondrial dysfunctions and slow the progression of HFpEF.

Methods

Animal experiments

Twenty 6-week-old male Dahl/SS rats (Charles River, China) were fed adaptively for one week. They were randomly divided into two groups. The heart failure group (HF) was fed with 8% NaCl high salt for 7 weeks, and the control group (C) was fed with 0.3% NaCl low salt for 7 weeks, with 4 rats in each group. The animals are kept in the Laboratory Animal Center of Shanghai Jiao Tong University and housed at 21–25 ℃, with 40–50% humidity, a 12 h light: 12 h dark cycle, and free access to drinking water and eating standard feed. After feeding, ultrasonic testing was performed, and the body weight (BW) was weighed. The rat was euthanized by cervical dislocation after inhalation anesthesia with isoflurane gas (concentration 5%, gas flow 500 ml/min). The rat heart was taken and the weight of heart and LV were weighed after termination. All experiments were performed in accordance with Chinese National and Shanghai Jiao Tong University ethical guidelines regarding the use of animals in research, consistent with the NIH guidelines (Guide for the care and use of laboratory animals) on the protection of animals used for scientific purposes. The experimental protocol was approved by the Animal Care and Use Committee of Shanghai Jiao Tong University, China.

PINK1 was specifically overexpressed by AAV in vivo

The cDNA encoding PINK1 was cloned into the myocardial specific overexpression plasmid pLV [Exp] - cTnT (myocardial specific promoter, vectorbuilder, China), and packaged with adeno-associated virus (AAV). The serotype is AAV9. After a week of adaptive feeding of 6-week-old male Dahl/SS rats, AAV was slowly injected into rats through the caudal vein, 1×10^{12} vg, followed by 7 weeks of high salt feeding. This resulted in PINK1 myocardial specific overexpression heart failure rats (HP); Control rats (C) and heart failure rats (HF) were injected with empty AAV, with 4 rats in each group.

Echocardiography

Cardiac structure and function were determined using the VEVO 3100 high-resolution micro ultrasound system. After animals were anesthetized with isoflurane (concentration 5%, gas flow 500 ml/min), they were placed on the heating table in a supine position. Left ventricular end systolic internal diameter (LVIDs), LV end diastolic internal diameter (LVIDd), interventricular septal end systolic thickness (IVSs), interventricular septal end diastolic thickness (IVSd), LV end systolic volume (ESV) and LV end diastolic volume (EDV) were measured by the M-mode ultrasound, based on which ejection fraction (EF) and fraction of shorten (FS) were calculated; The ratio of early diastolic maximum velocity of mitral valve to systolic maximum velocity of atrium (E/A) was measured by the blood flow Doppler mode; The ratio of the maximum velocity of blood flow in the early diastolic phase of mitral valve to the motion velocity of mitral annulus (E/E') was measured by the tissue Doppler mode.

Transmission electron microscope

The LV apical tissue was taken and fixed with 2.5% glutaraldehyde overnight. The heart was removed and post fixed in a mixture of 0.8% potassium ferrocyanide and 2% osmium tetroxide in 0.1 M sodium cacodylate buffer for 2 h. The area and number of mitochondria were observed by transmission electron microscope (Talo L120C G2). The decrease of mitochondrial number and the increase of mitochondrial area denoted the decrease of mitochondrial fission. The shooting times are 4300 X and 13500 X. Each

sample is photographed and analyzed with more than 5 visual fields and more than 100 mitochondria. The mitochondrial area is computed by ImageJ software.

H&E and Picro Sirius Red Staining

The isolated LV was fixed with 4% paraformaldehyde (China National Pharmaceutical Group Corporation), embedded in paraffin, and sectioned to a thickness of 4 um with a microtome (Leica RM2265, Germany). After dewaxing, sections were stained with hematoxylin-eosin or Picro Sirius Red. Cell area and collagen fiber area were analyzed by ImageJ software.

Culture of H9C2 cardiomyocyte line and lentivirus transfection

H9C2 cardiomyocyte line was purchased from the National Collection of Authenticated Cell Cultures, China. The cells were cultured in DMEM medium (Gibco) supplemented with 10% fetal bovine serum and in an environment of 37°C, 5% CO_2 and 95% air.

$PINK1^{KO}$ cells were generated by CRISPR/Cas9 system. PINK1 gRNA sequence: 5'-CCCGCACCACGAACTGCCGC-3', which was cloned into knockout plasmid pLV [CRISPR] (vectorbuilder, China), and then packaged with lentivirus. In normal medium, lentivirus was transfected into H9C2 cardiomyocytes for 24 hours to obtain $PINK1^{KO}$ cells. Control cells (C) were transfected with empty lentivirus.

Production of $Drp1^{WT}$ cells: the cDNA encoding Drp1 was cloned into the overexpression plasmid pLV [Exp] (vectorbuilder, China), and then packaged with lentivirus. In normal medium, lentivirus was transfected into $PINK1^{KO}$ cells for 24 hours to obtain $Drp1^{WT}$ cells. Primer sequence of Drp1 cDNA: Drp1-F: 5'- CGCGGATCCGCCACCATGGAGGCGCTGATCC-3'; Drp1-R: 5'-CCGCTCGAGTCACCAAAGATGAGTCTCTCG-3'.

Production of $Drp1^{S616A}$ cells: $Drp1^{S616A}$ mutates TCT at Drp1 S616 site into GCT (alanine). The cDNA encoding $Drp1^{S616A}$ was cloned into the overexpression plasmid pLV [Exp] (vectorbuilder, China), and then packaged with lentivirus. In normal medium, lentivirus was transfected into pink1ko cells for 24 hours to obtain $Drp1^{S616A}$ cells. The method of obtaining $Drp1^{S616A}$ cDNA is as follows: using common cDNA as template, the first half of the target gene is obtained by using primers Drp1-1F: 5'-CGCGGATCCGCCACCATGGAGGCGCTGATCC-3', Drp1-1R: 5'-GGCAGCCAGTTTTCGTG-3'. The second half of the target gene was obtained by primers Drp1-2F: 5'-CTGGCTGCCCGAGAAC-3', Drp1-2R: 5'-CCGCTCGAGTCACCAAAGA-TGAGTCTCTCG-3'. Using the above product as the template, the cDNA of $Drp1^{S616A}$ was obtained by using primers Drp1-F: 5'-CGCGGATCCGCCACCATGGAGGCGCTGATCC-3', Drp1-R: 5'- CCGCTCGAGTCACCAAAGATGAGTCTCTCG – 3'.

Real-time PCR

The LV was weighed (40 mg), cut, and placed in a 2 ml centrifuge tube, and 1 ml Trizol (Invitrogen) was added to extract RNA (if the sample was 6-well plate cells, use 500 ul Trizol to extract RNA). cDNA synthesis was performed according to the instruction of the RevertAid™ First-Strand cDNA Synthesis Kit. The primers were synthesized by Sangon Biotech (Shanghai) Co., Ltd (Tables S1). Amplification was performed using a real-time PCR instrument (ABI StepOnePlus Real Time PCR System 7500, USA). The reaction conditions were as follows: 95°C for 10 min then 40 cycles of denaturation at 95°C for 15 s and 60°C for 1 min.

Separation of mitochondrial protein and cytoplasmic protein

Take 50 mg LV tissue, and separate mitochondrial protein and cytoplasmic protein according to the process of mitochondrial separation Kit (Beyotime Biotechnology). After the sample was washed with the precooled PBS, mitochondrial separation reagent was added and homogenized; 1000 g of supernatant was centrifuged for 5 min to remove the precipitation, 11000 g of supernatant was centrifuged for 10 min to obtain mitochondrial precipitation, and the remaining supernatant was cytoplasmic protein.

Western blot

LV tissue (20 mg) was lysed with Ripa lysate (Beyotime Biotechnology) and the total protein was extracted. SDS-PAGE electrophoresis and membrane transfer were performed. Primary antibodies: Drp1 (1:1000, Abcam, UK), Drp1^{S616} (1:1000, CST, USA), PINK1 (1:1000, CST, USA), β-actin (1:1000, protein, USA), voltage dependent anion channel protein 1 (VDAC1, 1:1000, Immunoway, China). The strips were exposed with Fusion FX automatic chemiluminescence/fluorescence image analysis system, and the gray value of the strips was measured by ImageJ analysis software.

Immunofluorescence

The paraffin section was dewaxed and heated in a 95°C water bath for 20 min in sodium citrate antigen repair solution (Beyotime Biotechnology) and naturally cooled to room temperature (cell samples were fixed with 4% paraformaldehyde for 15 min). Sections or cells were blocked for 2 h at room temperature and incubated at 4°C for 20 h with primary antibodies against Drp1 (1:200, Abcam, UK) and mitochondrial preprotein translocases of the outer membrane (Tom20, 1:100, Santa Cruz, USA). After washing, they were incubated with Alexa Fluor 568 (1:1000, Jackson, USA) and Alexa Fluor 488 (1:1000, Jackson, USA) secondary antibodies for 1 hour at room temperature in the dark. After washing, they were incubated with DAPI (Beyotime Biotechnology) for 5 min. Sections or cells were imaged with a confocal microscope (Olympus Fluoview FV1000). Take more than 5 pictures for each sample. Cell samples were taken with more than 30 cells in each group. In each image, the ImageJ plug-in Coloc 2 was used to detect the Manders co-localization Coefficient (MCC) and to evaluate the co-localization of mitochondria and Drp1.

Morphological analysis of mitochondria

The cells were inoculated into the culture dish for overnight culture and washed twice with PBS. The culture containing 100 nM Mito-Tracker Red (Beyotime Biotechnology) was added. The cells were incubated at 37°C for 20 min and washed with PBS for 3 times. After replacing the culture medium, fluorescence images were obtained with the confocal microscope (Olympus Fluoview FV1000). More than 30 cells were photographed in each group. The mitochondrial aspect ratio was analyzed by ImageJ software to evaluate mitochondrial fission. The increase of aspect ratio indicates the prolongation of mitochondria, which is a sign of the decrease of mitochondrial fission.

Mitochondrial membrane potential

Mitochondrial membrane potential was detected by tetramethylrhodamine ethyl ester (TMRE) kit (Beyotime Biotechnology). The cells were inoculated into the Petri dish for overnight culture, washed twice with PBS, and incubated at 37°C with TMRE working solution for 15 min. The preheated medium was washed twice. After replacing the new medium, the fluorescence image was taken with the confocal microscope. More than 30 cells were photographed in each group. The fluorescence intensity of mitochondrial membrane potential was analyzed by ImageJ software.

ATP content detection

Take 20 mg of LV tissue or an equal amount of 6-well plate cells to detect the ATP content according to the process of ATP detection kit (Beyotime Biotechnology). The sample was homogenized after adding 200 ul lysate and centrifuged at 12000 g for 5min to obtain ATP. After adding ATP detection reagent, the sample luminous intensity was analyzed by chemiluminescence instrument to detect the ATP content. The protein concentration was detected. The ATP content of each sample was standardized through the protein concentration to obtain the relative content of ATP.

Statistical analysis

The two groups of data were analyzed by the independent sample t-test. One-way ANOVA test was used for the data of 3 groups and above, and Bonferroni or Dunnett's T3 was used for pairwise comparison. $P < 0.05$ indicated the significant difference. All data were analyzed using SPSS Statistics V21.0 software and the results were expressed as the mean ± standard deviation (SD).

Non-standard Abbreviations And Acronyms

HFpEF: heart failure with preserved ejection fraction

HFrEF: heart failure with reduced ejection fraction

Drp1: dynamic related protein 1

PINK1: PTEN induced putative kinase 1

OPA1: optical atrophy 1

MFF: mitochondrial fission factor

Fis1: fission protein 1

S616: Ser 616

AAV: adeno-associated virus

LVIDs: Left ventricular end systolic internal diameter

LVIDd: left ventricular end diastolic internal diameter

IVSs: interventricular septal end systolic thickness

IVSd: interventricular septal end diastolic thickness

ESV: left ventricular end systolic volume

EDV: left ventricular end diastolic volume

EF: ejection fraction

FS: fraction of shorten

E/A: the ratio of early diastolic maximum velocity of mitral valve to systolic maximum velocity of atrium

E/E': the ratio of the maximum velocity of blood flow in the early diastolic phase of mitral valve to the motion velocity of mitral annulus

VDAC1: voltage dependent anion channel protein 1

Tom20: the mitochondrial preprotein translocases of the outer membrane 20

TMRE: tetramethylrhodamine ethyl ester

CS: citrate synthase

SDH: succinate dehydrogenase

PDH: pyruvate dehydrogenase

ATPase: ATP synthase

SIRT3: sirtuin 3

PGC-1α: peroxisome promoter activated receptor gamma coactivator-1 α

NRF-1: nuclear respiratory factor-1

Mfn1/2: mitofusin 1/2

Declarations

Ethics approval and consent to participate

All experiments were performed in accordance with Chinese National and Shanghai Jiao Tong University ethical guidelines regarding the use of animals in research, consistent with the NIH guidelines (Guide for the care and use of laboratory animals) on the protection of animals used for scientific purposes. The experimental protocol was approved by the Animal Care and Use Committee of Shanghai Jiao Tong University, China.

Consent for publication

Not applicable

Availability of data and materials

All data generated or analyzed during this study are included in this published article (and its supplementary information files).

Conflict of Interest

None declared.

Sources of Funding

This work is supported by the National Key Research and Development Program of China 2021YFA1000200 and 2021YFA1000203 (Y. Huo), National Natural Science Foundation of China Grant 11732001 (Y. Huo), and Shenzhen Science and Technology R&D Grant KQTD20180411143400981 (Y. Huo).

Authors' contributions

YH directed this study and helped to revise the manuscript. JS completed all experiments and writing the first manuscript. All authors read and approved the final manuscript.

Acknowledgments

We thank all participants of the study in The Shanghai Jiao Tong University.

References

1. Benjamin EJ, Blaha MJ, Chiuve SE, Cushman M, Das SR, Deo R, et al. Heart disease and stroke statistics-2017 update: A report from the american heart association. Circulation. 2017;135:e146–

603.
2. Chen YT, Wong LL, Liew OW, Richards AM. Heart failure with reduced ejection fraction (hfref) and preserved ejection fraction (hfpef): The diagnostic value of circulating micrornas. Cells. 2019;8.
3. Simmonds SJ, Cuijpers I, Heymans S, Jones EAV. Cellular and molecular differences between hfpef and hfref: A step ahead in an improved pathological understanding. Cells. 2020;9.
4. Withaar C, Meems LMG, Markousis-Mavrogenis G, Boogerd CJ, Sillje HHW, Schouten EM, et al. The effects of liraglutide and dapagliflozin on cardiac function and structure in a multi-hit mouse model of heart failure with preserved ejection fraction. Cardiovasc Res. 2021;117:2108–24.
5. Shah SJ, Kitzman DW, Borlaug BA, van Heerebeek L, Zile MR, Kass DA, et al. Phenotype-specific treatment of heart failure with preserved ejection fraction: A multiorgan roadmap. Circulation. 2016;134:73–90.
6. Schiattarella GG, Altamirano F, Kim SY, Tong D, Ferdous A, Piristine H, et al. Xbp1s-foxo1 axis governs lipid accumulation and contractile performance in heart failure with preserved ejection fraction. Nat Commun. 2021;12:1684.
7. Nagueh SF. Heart failure with preserved ejection fraction: Insights into diagnosis and pathophysiology. Cardiovasc Res. 2021;117:999–1014.
8. Kumar AA, Kelly DP, Chirinos JA. Mitochondrial dysfunction in heart failure with preserved ejection fraction. Circulation. 2019;139:1435–50.
9. Sun X, Alford J, Qiu H. Structural and functional remodeling of mitochondria in cardiac diseases. Int J Mol Sci. 2021;22.
10. Deng Y, Xie M, Li Q, Xu X, Ou W, Zhang Y, et al. Targeting mitochondria-inflammation circuit by beta-hydroxybutyrate mitigates hfpef. Circ Res. 2021;128:232–45.
11. Whitley BN, Engelhart EA, Hoppins S. Mitochondrial dynamics and their potential as a therapeutic target. Mitochondrion. 2019;49:269–83.
12. Boutry M, Kim PK. Orp1l mediated pi(4)p signaling at er-lysosome-mitochondrion three-way contact contributes to mitochondrial division. Nat Commun. 2021;12:5354.
13. Rovira-Llopis S, Banuls C, Diaz-Morales N, Hernandez-Mijares A, Rocha M, Victor VM. Mitochondrial dynamics in type 2 diabetes: Pathophysiological implications. Redox Biol. 2017;11:637–45.
14. Kalkhoran SB, Kriston-Vizi J, Hernandez-Resendiz S, Crespo-Avilan GE, Rosdah AA, Lees JG, et al. Hydralazine protects the heart against acute ischaemia/reperfusion injury by inhibiting drp1-mediated mitochondrial fission. Cardiovasc Res. 2022;118:282–94.
15. Tilokani L, Nagashima S, Paupe V, Prudent J. Mitochondrial dynamics: Overview of molecular mechanisms. Essays Biochem. 2018;62:341–60.
16. Jimah JR, Hinshaw JE. Structural insights into the mechanism of dynamin superfamily proteins. Trends Cell Biol. 2019;29:257–73.
17. Jin JY, Wei XX, Zhi XL, Wang XH, Meng D. Drp1-dependent mitochondrial fission in cardiovascular disease. Acta Pharmacol Sin. 2021;42:655–64.

18. Tanaka K. The pink1-parkin axis: An overview. Neurosci Res. 2020;159:9–15.
19. Wang N, Zhu P, Huang R, Wang C, Sun L, Lan B, et al. Pink1: The guard of mitochondria. Life Sci. 2020;259:118247.
20. Lin J, Chen K, Chen W, Yao Y, Ni S, Ye M, et al. Paradoxical mitophagy regulation by pink1 and tufm. Mol Cell. 2020;80:607–20 e612.
21. Xu Y, Tang Y, Lu J, Zhang W, Zhu Y, Zhang S, et al. Pink1-mediated mitophagy protects against hepatic ischemia/reperfusion injury by restraining nlrp3 inflammasome activation. Free Radic Biol Med. 2020;160:871–86.
22. Saito T, Hamano K, Sadoshima J. Molecular mechanisms and clinical implications of multiple forms of mitophagy in the heart. Cardiovasc Res. 2021;117:2730–41.
23. Han H, Tan J, Wang R, Wan H, He Y, Yan X, et al. Pink1 phosphorylates drp1(s616) to regulate mitophagy-independent mitochondrial dynamics. EMBO Rep. 2020;21:e48686.
24. Zhang W, Zhang H, Yao W, Li L, Niu P, Huo Y, et al. Morphometric, hemodynamic, and multi-omics analyses in heart failure rats with preserved ejection fraction. Int J Mol Sci. 2020;21.
25. Bing F, Wang X, Shen W, Li L, Niu P, Chen Y, et al. Inhalation of ultrafine zinc particles impaired cardiovascular functions in hypertension-induced heart failure rats with preserved ejection fraction. Front Bioeng Biotechnol. 2020;8:13.
26. Lam CSP, Voors AA, de Boer RA, Solomon SD, van Veldhuisen DJ. Heart failure with preserved ejection fraction: From mechanisms to therapies. Eur Heart J. 2018;39:2780–92.
27. Zhou B, Tian R. Mitochondrial dysfunction in pathophysiology of heart failure. J Clin Invest. 2018;128:3716–26.
28. Chan DC. Mitochondrial dynamics and its involvement in disease. Annu Rev Pathol. 2020;15:235–59.
29. Wu S, Lu Q, Wang Q, Ding Y, Ma Z, Mao X, et al. Binding of fun14 domain containing 1 with inositol 1,4,5-trisphosphate receptor in mitochondria-associated endoplasmic reticulum membranes maintains mitochondrial dynamics and function in hearts in vivo. Circulation. 2017;136:2248–66.
30. Shirakabe A, Zhai P, Ikeda Y, Saito T, Maejima Y, Hsu CP, et al. Drp1-dependent mitochondrial autophagy plays a protective role against pressure overload-induced mitochondrial dysfunction and heart failure. Circulation. 2016;133:1249–63.
31. Wang Y, Wang H, Zhuo Y, Hu Y, Zhang Z, Ye J, et al. Sirt1 alleviates high-magnitude compression-induced senescence in nucleus pulposus cells via pink1-dependent mitophagy. Aging. 2020;12:16126–41.

Figures

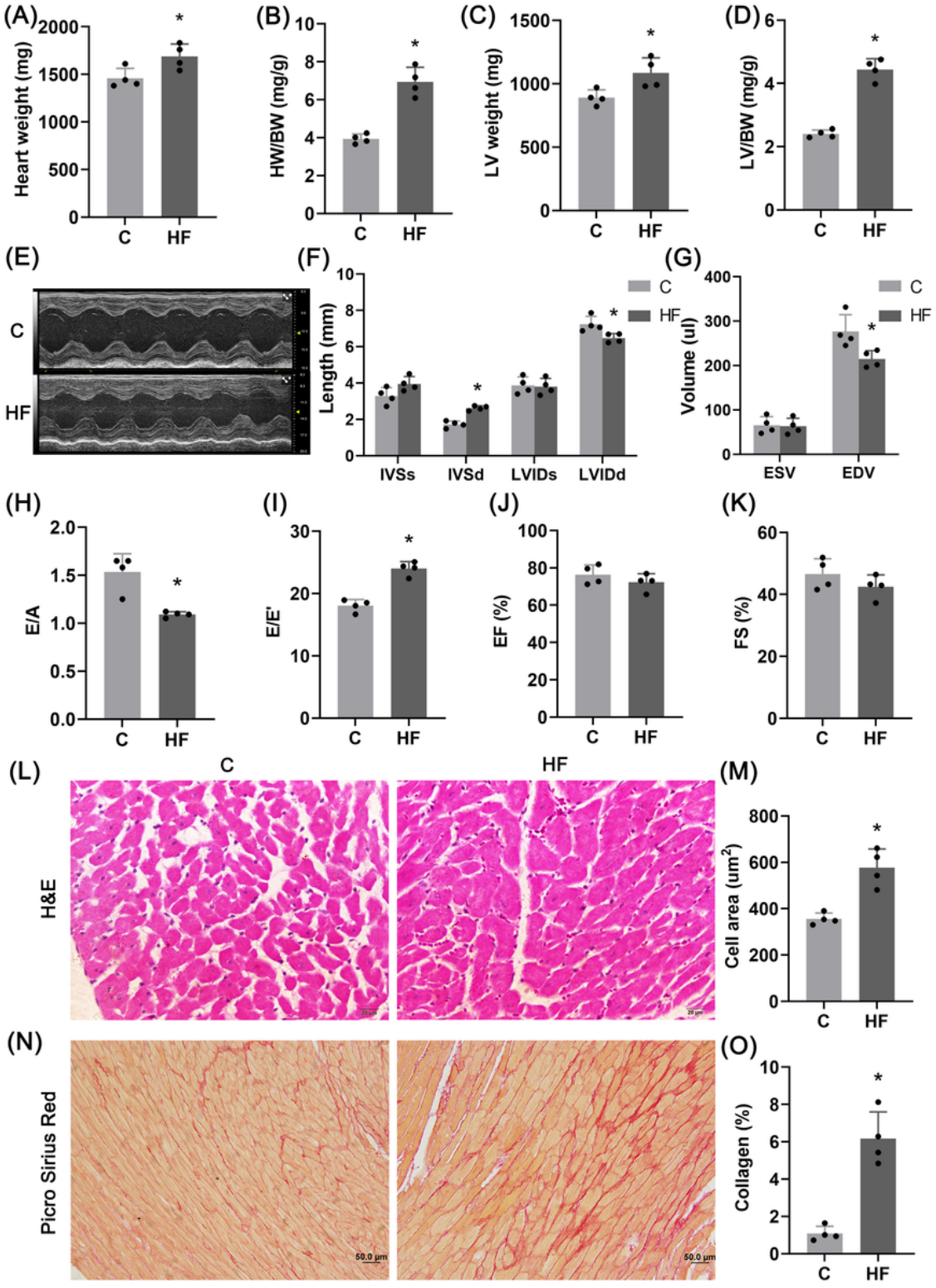

Figure 1

HFpEF model

(A-D) Heart weight (A), ratio of HW to BW (B), LV weight (C), and ratio of LV weight to BW (D); n=4 per group. (E-K) Representative images of M-mode ultrasound (E), interventricular septal end systolic thickness (IVSs), interventricular septal end diastolic thickness (IVSd), LV end systolic internal diameter

(LVIDs), LV end diastolic internal diameter (LVIDd) (F), end-systolic volume (ESV), end-diastolic volume (EDV) (G), E/A (H), E/E' (I), ejection fraction (EF) (J), and fraction of shorten (FS) (K); n=4 per group. (L, M) Representative images of LV H&E staining (L) and quantitative analysis of myocardial cell area (4 samples per group, 3-5 fields of view per sample, Scale bar: 20 μm) (M). (N, O) Representative images of Picro Sirius Red staining (N) and quantitative analysis of collagen fiber area fraction (4 samples per group, 3-5 fields analyzed per sample, Scale bar: 50 um) (O). The data are mean ± SD, * Compared with the C group, P <0.05.

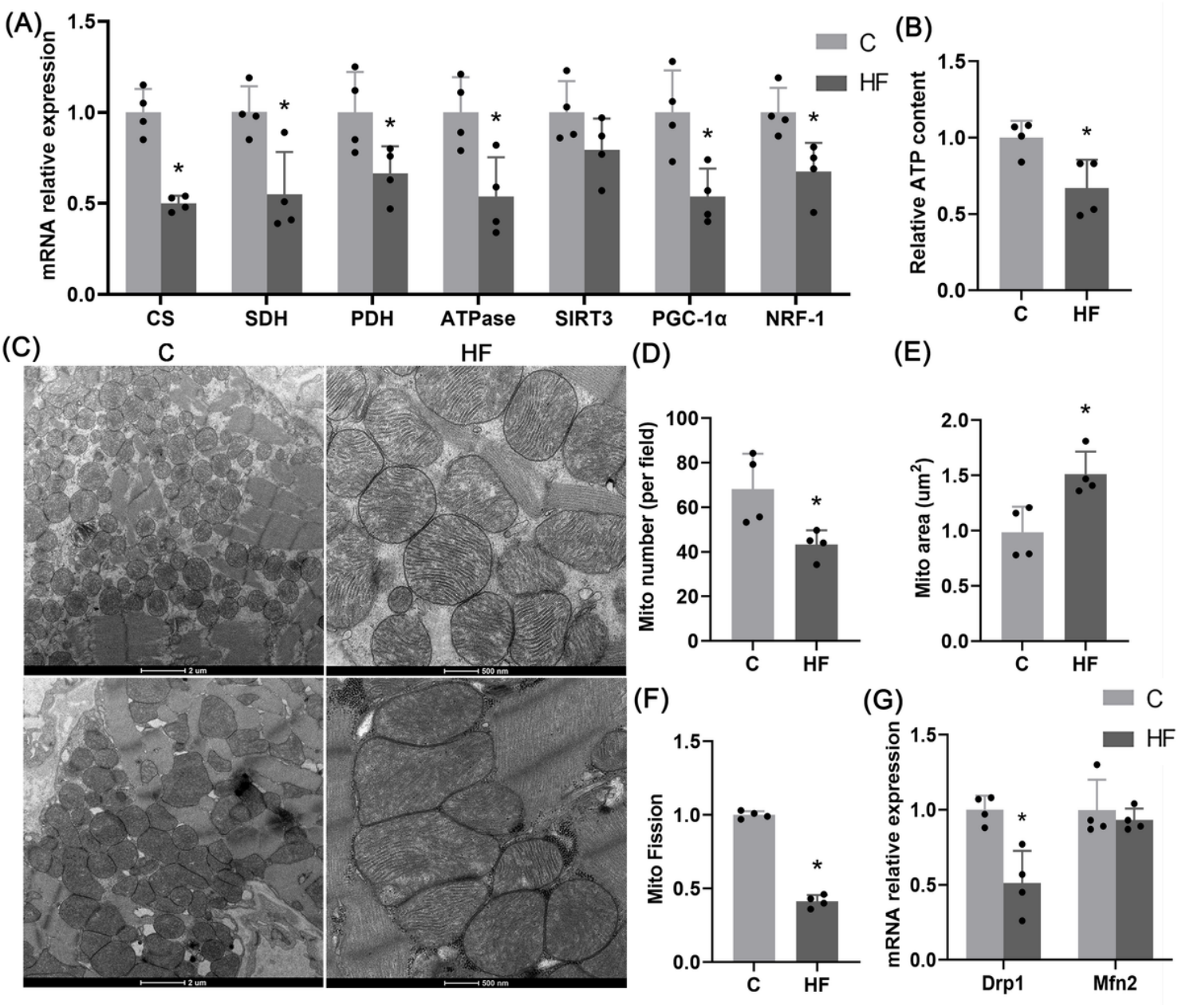

Figure 2

Mitochondrial dysfunctions in HFpEF

(A) mRNA expression of mitochondrial function-related genes CS, SDH, PDH, ATPase, SIRT3, PGC-1α, NRF-1 in the LV; n=4 per group. (B) Relative ATP content in the LV (normalized using protein concentration); n=4 per group. (C-F) Representative images of mitochondrial transmission electron microscopy in the LV (Scale bar: 2 um, 500 nm) (C), quantitative analysis of the number of mitochondria per unit field of view (analysis of more than 100 mitochondria per sample, 4 samples per group) (D), quantitative analysis of mitochondrial area (analysis of more than 100 mitochondria per sample, 4 samples per group) (E), and quantitative analysis of mitochondrial fission index (ratio of mitochondrial number to mitochondrial area, n = 4 per group) (F). (G) mRNA expression of Drp1, a key gene for mitochondrial fission in the left ventricle of rats, and Mfn2, a key gene for mitochondrial fusion (n=4 in each group). The data are mean ± SD, * Compared with the C group, P <0.05.

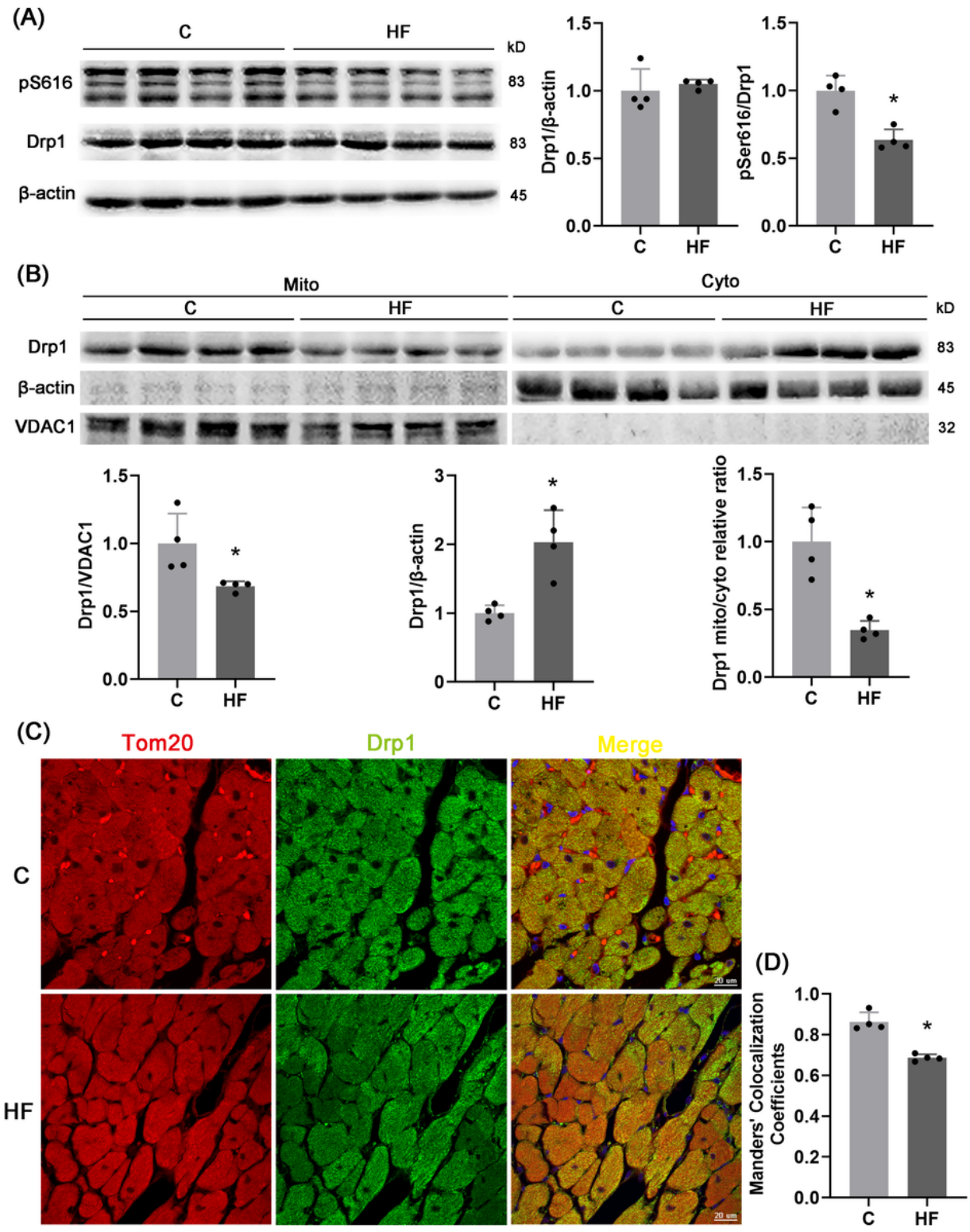

Figure 3

pDrp1^{S616}-mediated mitochondrial fission

(A) WB analysis of total protein levels of Drp1 and phosphorylation of Drp1^{S616} in the LV; n=4 per group. (B) Drp1 protein level on mitochondria, Drp1 protein level in cytoplasm, and relative ratio of mitochondrial Drp1 to cytoplasmic Drp1 after the separation of LV mitochondria and cytoplasmic proteins; n = 4 per

group. (C) Representative images of immunofluorescence of the LV (red: mitochondrial outer membrane marker, Tom20, green: Drp1, blue: DAPI, Scale bar: 20 um), and (D) Manders co-localization Coefficient (MCC) quantitative analysis of Tom20 and Drp1 (5 fields analyzed per sample, 4 samples per group). The data are mean ± SD, * Compared with the C group, P <0.05.

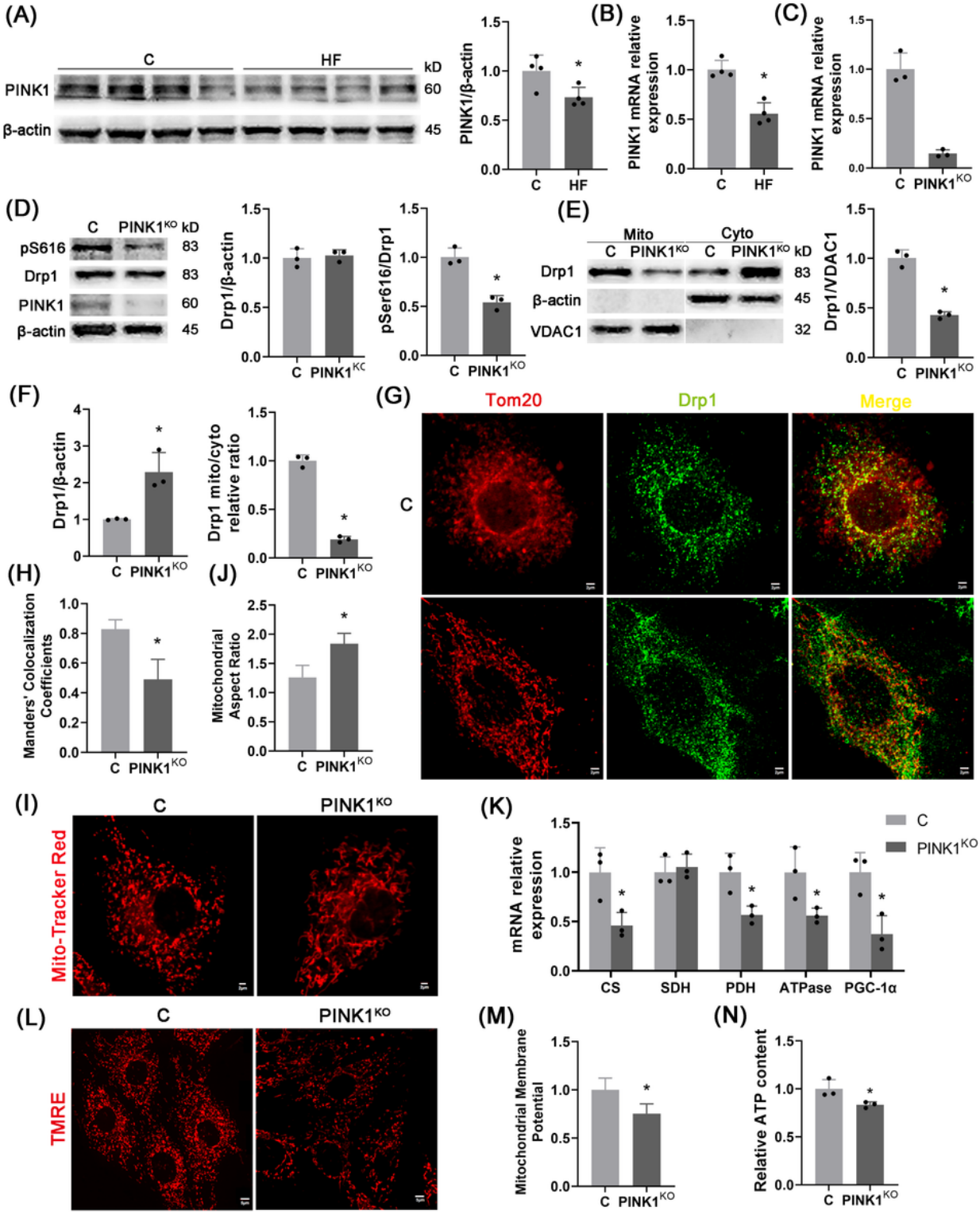

Figure 4

PINK1 knockout in H9C2 cardiomyocytes impairs mitochondrial fission and function

(A, B) PINK1 protein expression (A) and mRNA expression (B) in the LV; n=4 per group. (C, D) PINK1 mRNA expression (C) and PINK1 protein expression, Drp1 total protein level and $Drp1^{S616}$ phosphorylation level (D) in H9C2 cardiomyocytes after PINK1 knockout; n=3 per group. (E, F) Drp1 protein level on mitochondria (E) and Drp1 protein level in cytoplasm and relative ratio of mitochondrial Drp1 to cytoplasmic Drp1 (F) after separation of mitochondrial and cytoplasmic proteins of H9C2 cardiomyocytes; n=3 per group. (G, H) Representative images of immunofluorescence of H9C2 cardiomyocytes (red: mitochondrial outer membrane marker, Tom20, green: Drp1, blue: DAPI, Scale bar: 2 Um) (G) and Manders co-localization Coefficient (MCC) quantitative analysis of Tom20 and Drp1 (more than 30 cells were analyzed per group) (H). (I, J) Representative images of Mito-Tracker Red fluorescent staining of mitochondrial morphology (Scale bar: 2 um) (I) and quantitative analysis of mitochondrial aspect ratio (more than 30 cells analyzed per group) (J). (K) mRNA expression of mitochondrial function-related genes CS, SDH, PDH, ATPase, and PGC-1α in H9C2 cardiomyocytes, n=3 per group. (L, M) Representative images of TMRE mitochondrial membrane potential fluorescence staining (Scale bar: 5 um) (L) and quantitative analysis of mitochondrial membrane potential fluorescence intensity (more than 30 cells analyzed per group) (M). (N) Relative ATP content of H9C2 cardiomyocytes (normalized using protein concentration, n=3 per group). The data are mean ± SD, * Compared with the C group, $P < 0.05$.

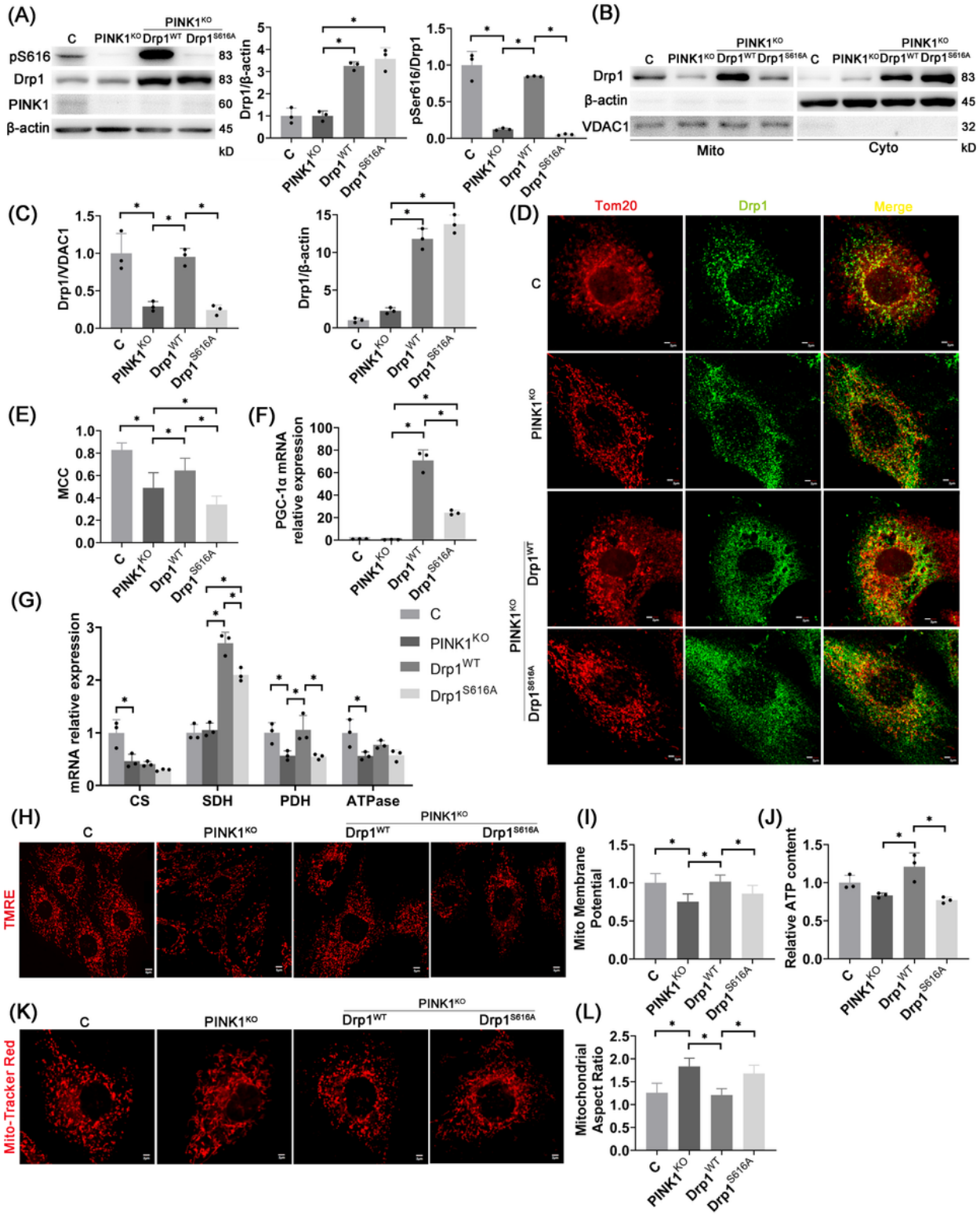

Figure 5

Overexpression of Drp1^{WT}, rather than Drp1^{S616A}, improve mitochondrial fission and function

(A) PINK1 protein expression, Drp1 total protein level and Drp1^{S616} phosphorylation level after PINK1^{KO} cardiomyocytes overexpressed Drp1^{WT} or Drp1^{S616A}; n=3 per group. (B, C) Drp1 protein levels on mitochondria and in cytoplasm after separation of mitochondrial and cytoplasmic proteins of H9C2

cardiomyocytes; n=3 per group. (D, E) Representative images of immunofluorescence of H9C2 cardiomyocytes (red: mitochondrial outer membrane marker, Tom20, green: Drp1, blue: DAPI, Scale bar: 2 um) (D) and Manders co-localization Coefficient (MCC) quantitative analysis of Tom20 and Drp1 (more than 30 cells analyzed per group) (E). (F, G) mRNA expression of mitochondrial function-related gene PGC-1α (F) and CS, SDH, PDH, ATPase (G) in H9C2 cardiomyocytes, n=3 per group. (H, I) Representative images of TMRE mitochondrial membrane potential fluorescence staining (Scale bar: 5 um) (H) and quantitative analysis of mitochondrial membrane potential fluorescence intensity (more than 30 cells were analyzed per group) (I). (J) Relative ATP content of H9C2 cardiomyocytes (normalized using protein concentration, n=3 per group). (K, L) Representative images of Mito-Tracker Red fluorescent staining of mitochondrial morphology (Scale bar: 2 um) (K) and quantitative analysis of mitochondrial aspect ratio (more than 30 cells analyzed per group) (L). The data are mean ± SD, *P < 0.05 compared to the other group.

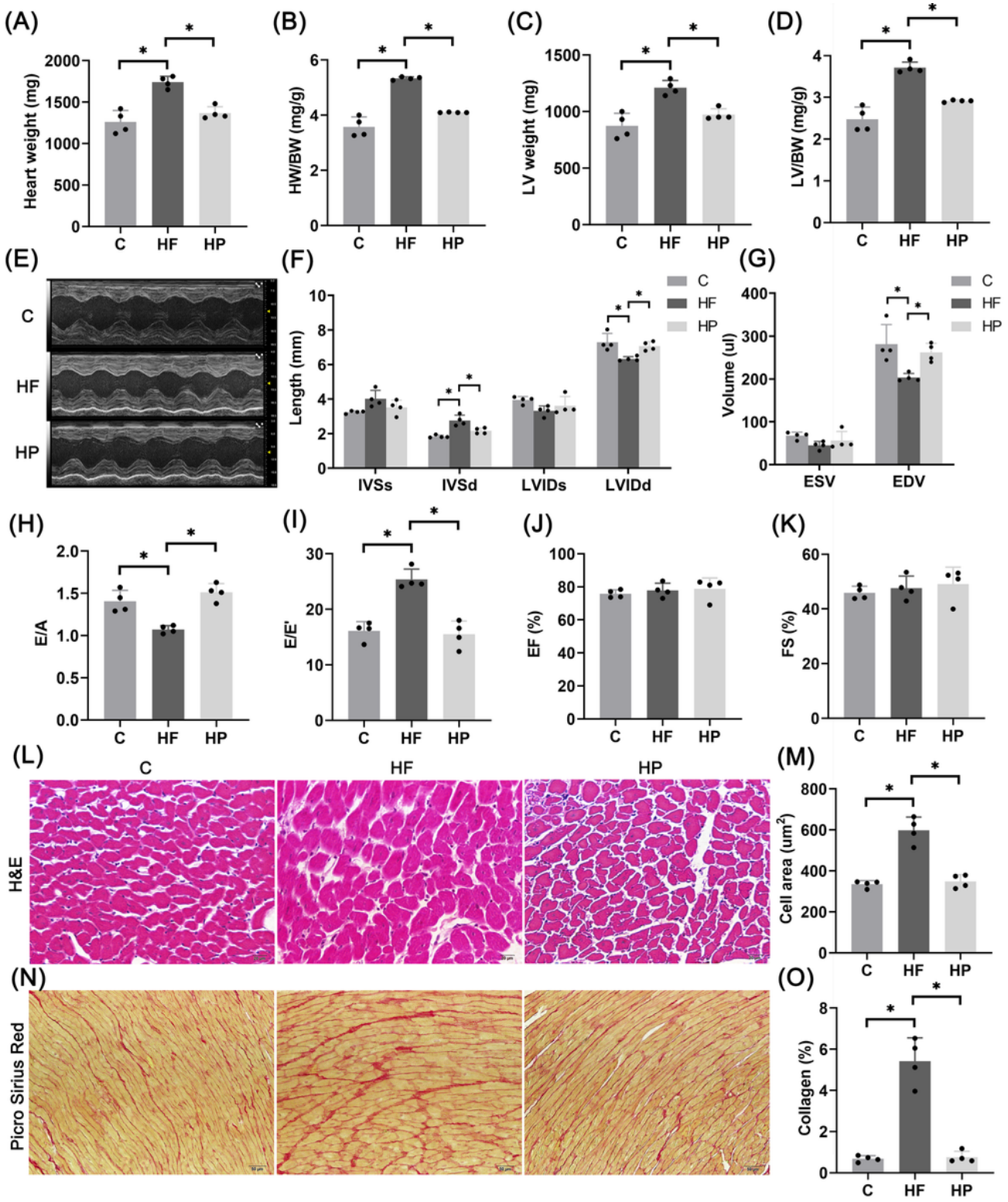

Figure 6

PINK1 overexpression improves HFpEF phenotypes

(A-D) Heart weight (A), ratio of heart weight to body weight (B), left ventricle weight (C), and ratio of left ventricle weight to body weight (D); n=4 per group. (E-K) Representative images of M-mode ultrasound (E), IVSs, IVSd, LVIDs, LVIDd (F), ESV, EDV (G), E/A (H), E/E' (I), EF (J), and FS(K); n = 4 per group. (L, M)

Representative images of H&E staining of rat left ventricle (L) and quantitative analysis of myocardial cell area (4 samples per group, 3-5 fields of view per sample, Scale bar: 20 um) (M). (N, O) Representative images of Picro Sirius Red staining (N) and quantitative analysis of collagen fiber area fraction (4 samples per group, 3-5 fields analyzed per sample, Scale bar: 50 um) (O). The data are mean ± SD, *P < 0.05 compared to the other group.

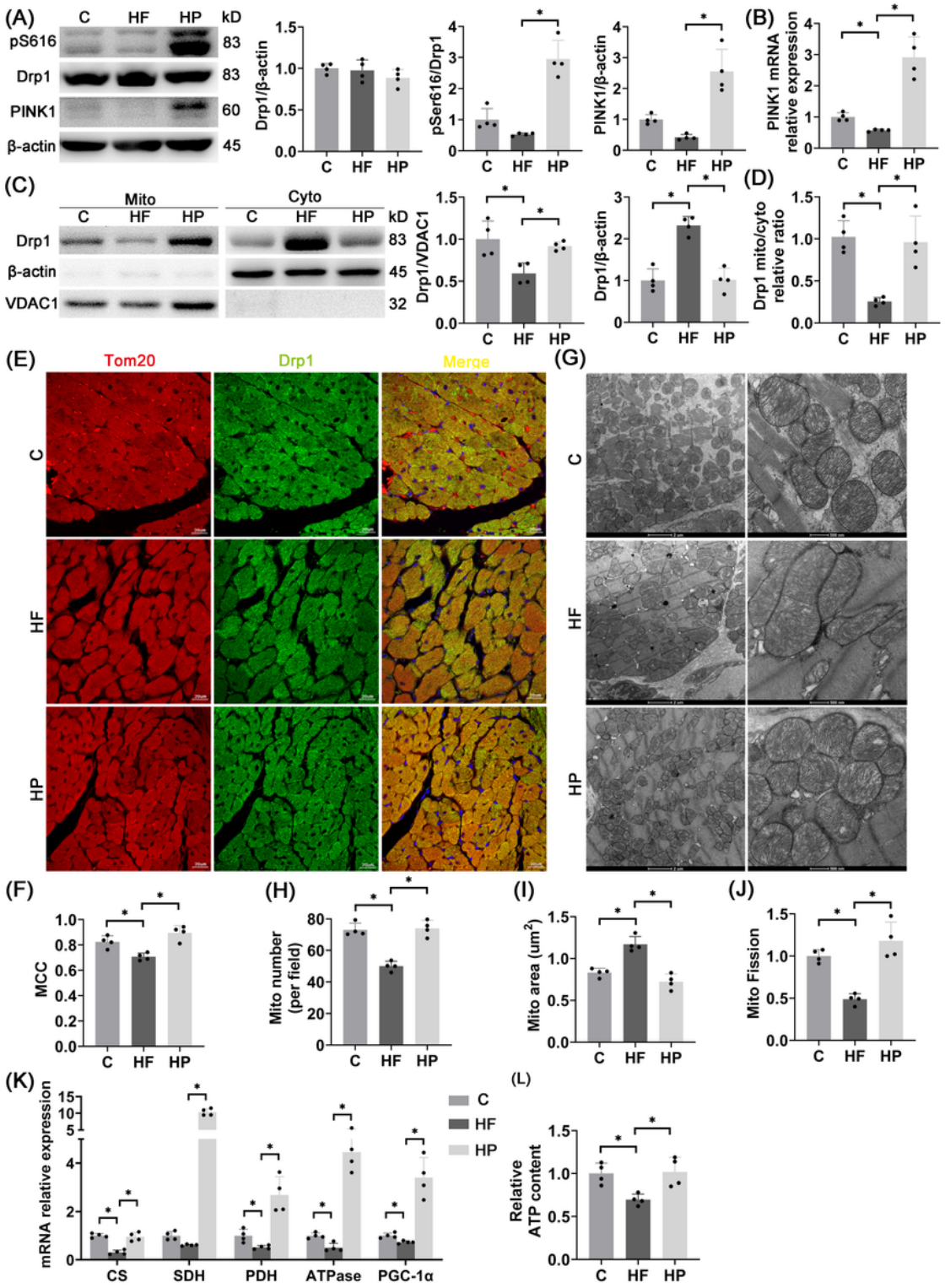

Figure 7

PINK1 overexpression stimulates pDrp1^{S616}-mediated fission to improve mitochondrial function

(A) Drp1 total protein expression, Drp1^{S616} phosphorylation level, and PINK1 protein expression in the LV; n=4 per group. (B) PINK1 mRNA expression in the LV; n=4 per group. (C, D) Drp1 protein level on mitochondria, Drp1 protein level in cytoplasm (C) and the relative ratio of mitochondrial Drp1 to cytoplasmic Drp1 (D) after the separation of LV mitochondria and cytoplasmic proteins; n =4 per set. (E, F) Representative images of immunofluorescence of the LV (red: mitochondrial outer membrane marker, Tom20, green: Drp1, blue: DAPI, Scale bar: 20 um) (E) and Manders co-localization Coefficient (MCC) quantitative analysis of Tom20 and Drp1 (5 fields analyzed per sample, 4 samples per group) (F). (G-J) Representative images of mitochondrial transmission electron microscopy in the LV (Scale bar: 2 um, 500 nm) (G) and quantitative analysis of the number of mitochondria per unit field of view (analysis of >100 mitochondria per sample, 4 samples per group) (H), quantitative analysis of mitochondrial area (more than 100 mitochondria analyzed per sample, 4 samples per group) (I), and quantitative analysis of mitochondrial fission index (ratio of mitochondrial number to mitochondrial area, n=4 per group) (J). (K) mRNA expression of mitochondrial function-related genes CS, SDH, PDH, ATPase and PGC-1α in the LV; n=4 per group. (L) Relative ATP levels in rat hearts (normalized using protein concentration); n=4 per group. The data are mean ± SD, *P < 0.05 compared to the other group.

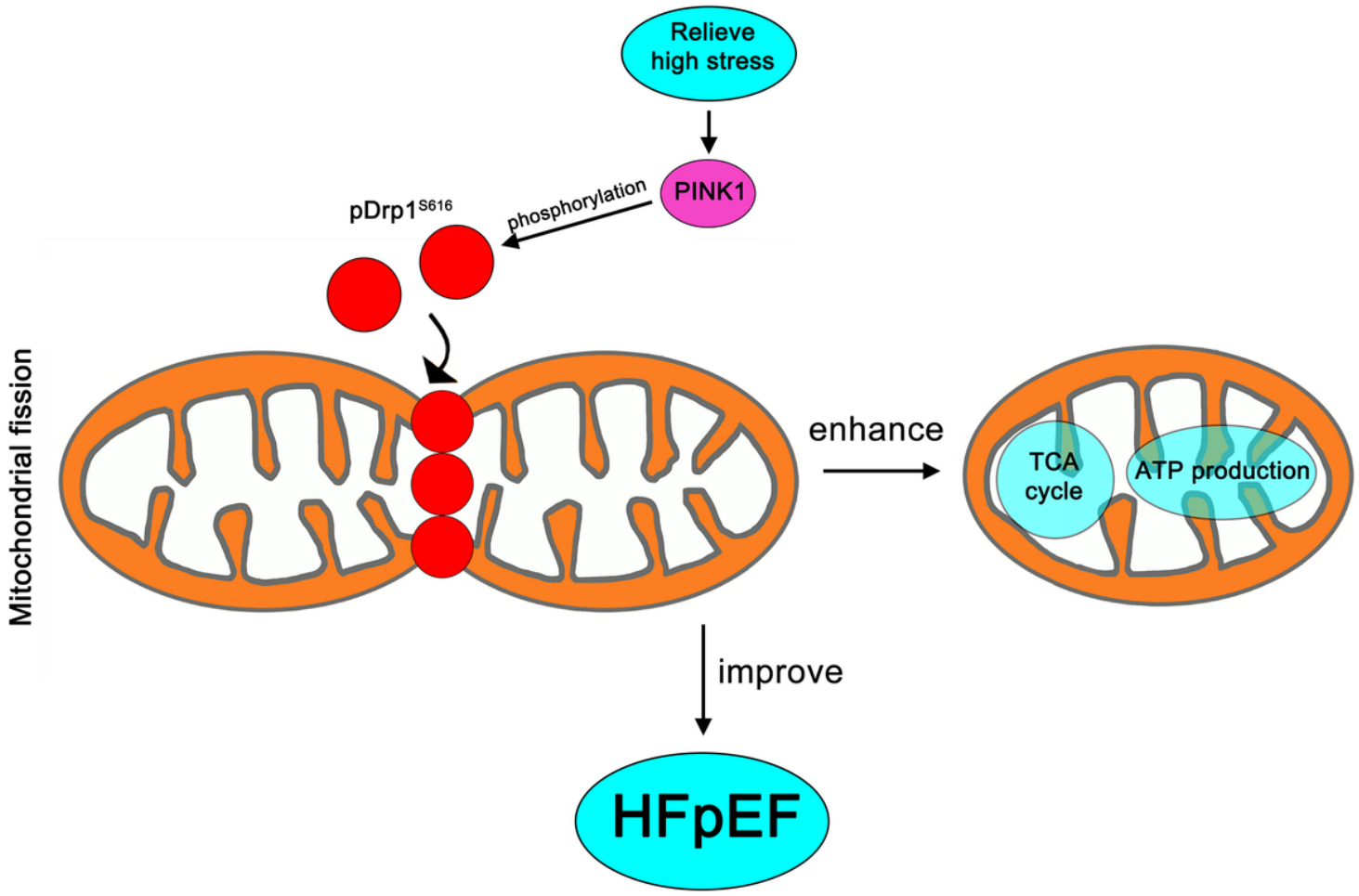

Figure 8

Molecular mechanism of PINK1-regulated HFpEF

PINK1 increases phosphorylation level of $Drp1^{S616}$ and mitochondrial localization of Drp1 to stimulate mitochondrial fission, thereby restoring mitochondrial function and ultimately slowing the development of HFpEF.

Supplementary Files

This is a list of supplementary files associated with this preprint. Click to download.

- SupplementalData.pdf
- Supplementaltable1.pdf